

# Experimental and Numerical Study of Asymmetric Vortex Merger in a Pure Electron Plasma

M. Amoretti\*, D. Durkin<sup>†</sup>, J. Fajans<sup>†</sup>, R. Pozzoli\* and M. Romé\*

*\*I.N.F.M. (U.d.R. Milano Università) and Dipartimento di Fisica, Università degli Studi di Milano,  
Via Celoria 16, 20133 Milano, Italy*

*<sup>†</sup>Department of Physics, University of California at Berkeley, Berkeley, California 94720-7300*

**Abstract.** The merging of an intense localized vortex with an extended vortex is investigated by means of an experimental analysis performed on a Malmberg-Penning trap with photocathode, and numerical simulations with a two-dimensional (2D) particle in cell (PIC) code. The study is restricted to highly nonlinear conditions, where the perturbative approach does not hold. A very good agreement between experimental results and simulations is obtained. It is found that the localized vortex is firstly wrapped around by the extended vortex, then moves towards the center of the system, eventually approaching an almost stationary state of rotation characterized by the formation of vorticity holes. During the whole evolution the extended vortex gains energy from the field surrounding the vortices, while the energy of the localized vortex remains constant.

## INTRODUCTION

Under suitable conditions, the dynamics perpendicular to the imposed magnetic field of a pure electron plasma confined in a Malmberg-Penning trap is equivalent to that of a 2D incompressible, inviscid fluid [1], where the vorticity  $\zeta$  is proportional to the 2D electron density  $n$ . This fact allows to investigate on such a system nonlinear processes occurring in 2D inviscid flows; in particular vortex merger and filamentation, which play a dominant role in the evolution of turbulence [2].

We consider here the process of interaction between an extended vortex and one very localized vortex (almost pointlike) under conditions, which have now become experimentally accessible, where the existing perturbative analysis [3] does not apply. The experimental investigation of this process is performed on a Malmberg-Penning trap (see Fig. 1) with photocathode [4], which allows to produce well-defined and well-localized vortices of almost uniform vorticity. The interpretation of the process is based on the Hamiltonian character of the motion, and numerical simulations with the 2D (in real space) PIC code XOOPIC [5].

Numerical investigations of the interaction of two isolated vortices of uniform vorticity, were reported, e.g., in Refs. [6, 7, 8]. In Ref. [6], in particular, it was pointed out the possibility of a merger by “entrainment” of the larger-vorticity region within the smaller-vorticity region. In Ref. [8], all possible regimes of interaction were investigated, but assuming identical vorticity for the two vortices. These works were all based on contour dynamics simulations. In Ref. [7], based on the use of a low-order Hamiltonian moment

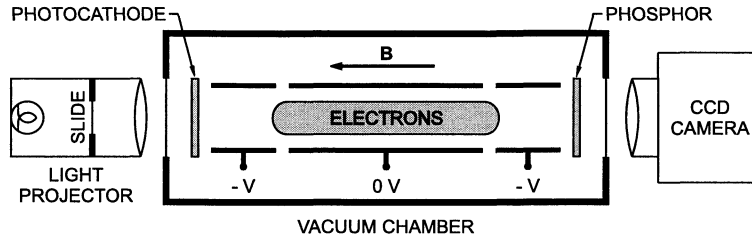


**FIGURE 1.** The Malmberg-Penning Trap with the photocathode [4]. The desired initial 2D electron distribution is created by projecting the appropriate light image onto a cesium antimonide photocathode and grounding the left cylinder; electrons are emitted only where there is light, and they stream along the magnetic field lines into the central confinement region, preserving their distribution.

model and a pseudospectral algorithm, it was pointed out how the interaction between two unequal vortices, of different size and vorticity, could cause one of the two vortices to dominate. In the language of Ref. [7], the case studied here corresponds to the smaller vortex being *victor*.

The dynamics of the system is described by the divergence-free velocity field  $\mathbf{u}(x, y, t) = \mathbf{e}_z \times \nabla \psi(x, y, t)$ , where the evolution of the stream function  $\psi$  is determined by the conservation of the vorticity  $\zeta \equiv \mathbf{e}_z \cdot \nabla \times \mathbf{u}$ ,

$$\partial \zeta / \partial t + [\zeta, \psi] = 0, \quad (1)$$

where  $[a, b] \equiv \partial a / \partial y \cdot \partial b / \partial x - \partial a / \partial x \cdot \partial b / \partial y$  is the Poisson bracket, the coordinates  $y, x$  are conjugate variables with respect to the Hamiltonian  $\psi$ , and

$$\nabla^2 \psi = \zeta. \quad (2)$$

The functions  $\psi$  and  $\zeta$  are related to the electric potential  $\phi$  and electron density  $n$  by the relations  $\phi = (B/c)\psi$  and  $n = (B/4\pi ec)\zeta$ , respectively, where  $B$  is the magnetic field strength and the other notations are standard. The evolution of the system is determined by appropriate initial and boundary conditions for  $\psi$ . In particular, the free-slip boundary condition  $\psi = 0$  on the circular wall corresponds to the condition  $\phi = 0$  for the electrostatic potential.

We refer to two initially circular vortices with uniform vorticities  $\zeta_e \ll \zeta_p$ , and initial radii  $a_e \gg a_p$  (the indices  $e, p$  denote the extended and the pointlike vortex, respectively). The experimentally investigated range of parameters in general corresponds to conditions, in which the initial field  $\psi$  exhibits a separatrix, with its X-point located outside the two vortices. Reference parameters can be taken  $\Gamma_p / \Gamma_e \approx 10^{-1}$ , with the initial distance  $d$  between the centers of the two vortices in the range  $1 + \Gamma_p / \Gamma_e < d / a_e < 2$ , with  $\Gamma_{e,p} = \pi \zeta_{e,p} a_{e,p}^2$  the circulation of the two vortices. A discussion of the characteristics of the merging process when the above parameters are varied is reported in Ref. [9].

In the cases under consideration the analysis which can be carried on, following Refs. [3, 10, 11], has a very narrow domain of validity since the shape of the extended vortex is soon highly distorted from its initial condition, the merging being very fast and lasting few rotation periods.

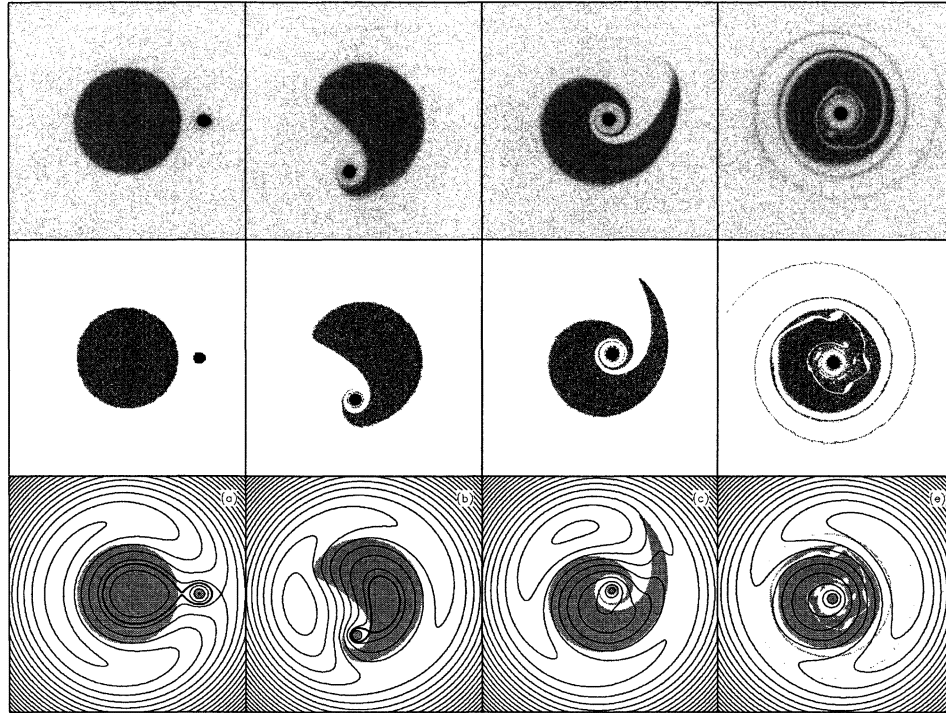


**FIGURE 2.** Time evolution of the interaction of a point vortex with an extended vortex. First row: density (experimental results). Second row: density (PIC simulation). Third row: contour plot of the corotating potential  $\bar{\psi}$  (PIC simulation): the thick line represents the separatrix crossing the extended vortex. The lengths are normalized over  $R_w$ . From left to right, the data refer to  $t = 0.0, 0.5, 1.0,$  and  $4.0,$  respectively, with the time measured in units of the period of rotation of the extended vortex,  $4\pi/\zeta_e$ .

Fig. 2 in the first row shows the experimentally detected images (the intensity is proportional to the axially integrated electron density) at different times of the evolution: from the initial condition to the final almost stationary state. The corresponding plots obtained by PIC simulations are shown in the second row of the same figure. The number  $N$  of macroparticles used in the simulations is  $\leq 10^5$  with a  $256 \times 256$  square grid. The parameters of the simulation are the same as in the experimental situation. The stability of the results with respect to variations of  $N$  and grid size has been verified.

The agreement between experimental data and simulation shows that the behavior of the system is indeed 2D Eulerian, even in this highly nonlinear regime; this confirms the potentiality of Malmberg-Penning traps for fluid dynamics experiments.

To describe the evolution of the system, we focus on the behavior of the stream function in a reference frame which rotates with the angular velocity,  $\omega$ , of the localized vortex,  $\bar{\psi} = \psi - \omega(x^2 + y^2)/2$ . The initial condition of the system appears far from the equilibrium, which is characterized by a vorticity field depending on the space variables only through  $\bar{\psi}$ . In the case under consideration, we chose a value of  $\omega$  corresponding

to the angular velocity of the localized vortex,  $\omega \simeq \Gamma_e/(2\pi d^2)$ . For high enough values of the ratio  $\Gamma_p/\Gamma_e$  (verifying the conditions mentioned above), a separatrix of the  $\bar{\psi}$  field exists, with an hyperbolic point located between the centers of the two vortices, as shown in the first plot in the third row of Fig. 2. Moreover, such separatrix crosses the extended vortex so that a finite part of it lies outside the separatrix: this part gives rise to the wrapping process.

The region enclosed by the separatrix around the localized vortex can be crossed by few fluid particles only, and forms a zero vorticity region which surrounds the localized vortex during the whole evolution of the system. This has been remarked also in the analysis of the motion of a localized vortex in a space dependent vorticity background [10]. The presence of the mentioned hyperbolic point determines the shape of the extended vortex during the initial phase of wrapping, as shown in the second plot, a key role being due to the different behavior of fluid particles in the neighborhood of that point. As wrapping develops, the related shift of the center of vorticity of the extended vortex feeds the process and leads to the coalescence of the hyperbolic point with the elliptic point associated to the extended vortex. Then,  $\bar{\psi}$  exhibits a single maximum in the region of interest, as shown in the last two plots.

The second phase of the motion is characterized by formation and stretching of filaments, and effective reconnection of the vorticity field with the related formation and stirring of holes, which occurs due to the Kelvin-Helmholtz instability arising in the spiral channel of zero vorticity inside the extended (constant vorticity) vortex [7]. During this process the  $\bar{\psi}$  field does not show significant large scale evolution. The constraint of vorticity conservation does not allow the system to reach a state where  $\zeta$  is a function of  $\bar{\psi}$  only.

Finally, we consider the behavior of the energy flows during the merger. The energy density is given by  $\varepsilon(x, y, t) = \frac{1}{2}|\nabla\psi|^2$ . This is initially concentrated near the boundaries of the two vortices, and it has a local minimum in the region around the above mentioned X-point. The total energy of the system,  $E$ , is a constant of motion and reads

$$E = \frac{1}{2} \int_S |\nabla\psi|^2 dS = \sum_i E_i, \quad (3)$$

where the integration is over the whole space within the circular boundary, and the energies  $E_i$ , with  $i = e, p, b$ , have been introduced, representing the energy associated to the extended vortex, the localized vortex, and the region surrounding the two vortices (background), respectively. The behavior of the energy amount in the two vortices and in the background is shown in Fig. 3, where the time evolution of the  $E_i$ 's is shown. During the whole process the energy of the pointlike vortex approximately does not change, while the energy of the extended vortex increases (almost linearly), at the expense of the energy of the background.

## ACKNOWLEDGMENTS

This work was partially supported by the Office of Naval Research, and by the Italian Ministry of Education and Scientific Research.

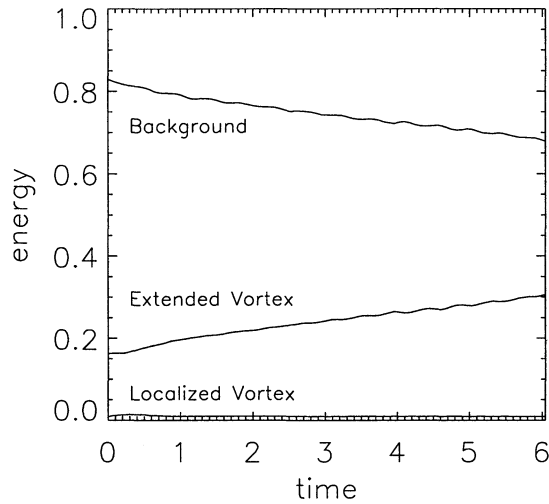


**FIGURE 3.** Time evolution of the total fluid energy of the two vortices and the background (PIC simulation). The data are the same as in Fig. 2.

## REFERENCES

1. R. H. Levy, *Phys. Fluids* **8**, 1288 (1965).
2. J. C. McWilliams, *J. Fluid Mech.* **219**, 361 (1990).
3. I. M. Lansky, T. M. O'Neil, and D. A. Schecter, *Phys. Rev. Lett.* **70**, 1479 (1997).
4. D. Durkin and J. Fajans, *Rev. Sci. Instrum.* **70**, 4539 (1999).
5. J. P. Varboncoeur, A. B. Langdon, and N. T. Gladd, *Comp. Phys. Comm.* **87**, 199 (1995).
6. E. A. Overman and N. J. Zabusky, *Phys. Fluids* **25**, 1297 (1982).
7. M. V. Melander, N. J. Zabusky, and J. C. McWilliams, *Phys. Fluids* **30**, 2610 (1987).
8. D. G. Dritschel and D. W. Waugh, *Phys. Fluids A* **4**, 1737 (1992).
9. M. Amoretti, D. Durkin, J. Fajans, R. Pozzoli, and M. Romé, *Phys. Plasmas* **8**, 3865 (2001).
10. D. A. Schecter and D. H. E. Dubin, *Phys. Rev. Lett.* **83**, 2191 (1999).
11. D. Z. Jin, Ph.D. thesis, University of California, San Diego, 1999.